### Title

Anti-plane shear waves in periodic elastic composites: band structure and anomalous wave refraction




### Journal

Proceedings of the Royal Society A, 471(2180)

### ISSN

1364-5021



### Author

Nemat-Nasser, Sia



### Publication Date

2015-08-01

### DOI

10.1098/rspa.2015.0152

Peer reviewed

# Anti-plane Shear Waves in Periodic Elastic Composites: Band Structure and Anomalous Wave-refraction

Sia Nemat-Nasser

*Department of Mechanical and Aerospace Engineering*
*University of California, San Diego*
*La Jolla, CA, 92093-0416 USA*

---

**Abstract**

For anti-plane shear waves in periodic elastic composites, it is shown that *negative energy refraction can be accompanied by positive phase-velocity refraction* and *positive energy refraction can be accompanied by negative phase-velocity refraction*, and that, this can happen over a broad range of frequencies. Hence, in general, negative refraction does not necessarily require antiparallel group and phase velocity vectors. Details are given for layered composites and the results are extended to, and illustrated for, two-dimensional periodic composites, revealing a wealth of information about the refractive characteristics of this class of composites. The composite's unit cell may consist of any number of constituents of any *variable mass-density and elastic modulus, admitting large discontinuities*.

A powerful variational-based solution-method is used that applies to one-, two-, and three-dimensional composites, whether their constituents are homogeneous or heterogeneous. The calculations are direct, accurate, and efficient, yielding the band structure, group-velocity, energy-flux, and phase-velocity vectors as functions of the frequency and wave-vector components,

over an entire frequency band.

*Keywords:*

Anti-plane shear waves, anomalous energy-flux and phase-velocity refraction, layered and doubly periodic composites

---

## 1. Introduction

Elastic composites can have remarkable mechanical and acoustic properties that are not shared by their individual constituents. They have found widespread applications and hence have been extensively studied; see for example [41, 8, 31, 5, 15]. Here the focus is on harmonic waves in periodic elastic composites, and their dynamic properties [40, 25, 21, 43]. In this context, efficient and accurate calculation of their band structure for Bloch-form harmonic waves is the necessary first step in estimating their overall response and effective dynamic constitutive properties [32, 33]. Various techniques have been used to study the dynamic responses of laminated composites; see [37] for a review of recent contributions. This includes, for example, methods such as direct analytic solutions for layered composites [36, 9, 20, 6]; transfer matrix [39, 12, 4, 16, 35, 10]; plane-wave expansion [24]; displacement-based variational methods [13, 14]; and finite elements [18, 1, 2]. Except for the last three methods, the other methods are limited to one-dimensional composites of homogeneous layers. The plane-wave expansion and the displacement-based variational methods (which lead to the same set of final equations) are inefficient, requiring thousands of terms to produce reasonably accurate results in the presence of large discontinuities (mass-density and stiffness) which is a common feature of this class of composites [17, 28].

To produce an effective tool that accounts for discontinuities as an integral part of the variational formulation, a mixed variational method has been developed and successfully used in the 1970's to calculate the band structure of one-, two-, and three-dimensional periodic elastic composites; [26, 27, 29, 22]. This mixed variational method yields very accurate results

and the rate of convergence of the corresponding approximating series solution is greater than that of the Rayleigh quotient with displacement-based approximating functions [3]. Since it is based on a variational principle, any set of approximating functions can be used for calculations, e.g., plane-waves Fourier series, as in the above cited papers, or finite elements [23].

The method has been revived in recent years and applied to calculate the effective overall dynamic constitutive parameters of periodic composites for Bloch waves traveling normal to the layers [33]. The limits of the accuracy of the resulting homogenized properties have been examined by considering the response of a layered composite interfaced with its homogenized half-space [38]; see also, [42].

When elastic waves are at an angle relative to an interface of a half-space layered composite, they generate a complex set of reflected and transmitted waves. It was recently suggested by Willis (personal communication, 2013) that this complexity is avoided by considering oblique anti-plane shear waves. This then allows the study of a number of physically interesting phenomena, such as negative refraction, within a relatively simple mathematical framework. Willis (personal communication, 2013) shows negative energy refraction when a layered composite is interfaced with a homogeneous solid on a plane normal to the layers. Here, we revisit this and in addition show that, unlike in metamaterials, such negative refraction is accompanied by positive phase-velocity refraction.

The calculation of the band structure, mode shapes, group-velocity, and energy-flux vectors in terms of the wave-vector components for a wide range of frequencies, is a challenging task. Here this problem is addressed, success-

fully formulated, and solved using a mixed variational method to calculate *the entire band structure and the associated mode shapes* for oblique anti-plane shear waves in layered elastic composites, and the results are extended to, and illustrated for, two-dimensional unit cells. *The composite may consist of periodically distributed unit cells of any number of constituents of any desired variable properties.* It is shown that composites with *two- and three-phase unit cells may display negative refraction*, which however is accompanied by *positive phase-velocity refraction.* Indeed, for layered composites, it is shown that *only the components of the phase and group velocities normal to the layers are antiparallel while the corresponding components along the layers are parallel.* This phenomenon is demonstrated by considering the refraction and reflection of plane waves when the composite is in contact with a homogeneous solid on a plane normal to the layers, as well as when the contact plane is parallel to the layers. In the first case, negative energy refraction with positive phase refraction occurs, and, in the second case, positive energy refraction with negative phase refraction occurs.

The calculations are direct and require no iteration, producing the entire band structure of the composites with unit cells of any number of constituents of any constant or variable properties. This also yields explicit series-form expressions for all the field variables necessary to calculate the components of the group-velocity and the energy-flux vectors, from which the overall response of the composite can readily be extracted.

When the phase-velocity and energy-flux vectors are antiparallel, the resulting waves have been called *backward waves* or BW [34, 19]. In general, backward waves and negative refraction occur when the wave-vector and the

energy-flux vector are antiparallel. Here, for the layered composite, we show *negative energy refraction* with *positive phase refraction*, that is, we show that only one component of the phase velocity is antiparallel with its corresponding component of the energy-flux (or group velocity) vector, while the other component of these vectors are parallel, leading to negative refraction with positive phase refraction. A similar phenomenon was first recognized to exist in photonic crystals by [11]. In addition, we show here that *negative phase refraction* can occur with *positive energy refracttion*.

## 2. Statement of the Problem and Field Equations

To present the general method, we first consider a layered composite and then extend the results to two-dimensional unit cells. Take the $x_1$-axis normal, and the $x_2$ and $x_3$ parallel to the layers. With $a$ denoting the length of a typical unit cell, the mass-density $\hat{\rho}$ and the elastic shear moduli, $\hat{\mu}_{jk}$, $j,k = 1,2$, with $\hat{\mu}_{12} = \hat{\mu}_{21}$, have the periodicity of the composite, i.e.,

$$\hat{\rho}(x_1) = \hat{\rho}(x_1 + ma); \quad \hat{\mu}_{jk}(x_1) = \hat{\mu}_{jk}(x_1 + ma), \quad j,k = 1,2, \tag{1}$$

for any integer m.

For Bloch-form time-harmonic anti-plane shear waves of frequency $\omega$ and wave-vector components $k_1$ and $k_2$, the nonzero displacement component $\hat{u}_3(x_1, x_2, t)$ has the following structure:

$$\hat{u}_3 = u_3^p(x_1) e^{i(k_1 x_1 + k_2 x_2 - \omega t)}, \tag{2}$$

where $u_3^p(x_1)$ is periodic with the periodicity of the unit cell.

Set

$$\xi_1 = x_1/a, \quad \xi_2 = x_2/a, \quad Q_1 = k_1 a \quad Q_2 = k_2 a, \tag{3}$$

introduce the average parameters,

$$\bar{\rho} = \int_{-1/2}^{1/2} \hat{\rho}(a\xi)d\xi, \quad \bar{\mu}_{11} = \int_{-1/2}^{1/2} \hat{\mu}_{11}(a\xi)d\xi, \tag{4}$$

and consider the following dimensionless quantities:

$$\begin{gathered} \mu_{jk}(\xi_1) = \hat{\mu}_{jk}(a\xi_1)/\bar{\mu}_{11}, \quad \rho(\xi_1) = \hat{\rho}(a\xi_1)/\bar{\rho}, \qquad \nu^2 = a^2\omega^2\bar{\rho}/\bar{\mu}_{11}, \\ w^p(\xi_1) = u_3^p(a\xi_1)/a, \qquad \tau_1 = \sigma_{13}/\bar{\mu}_{11}, \qquad \tau_2 = \sigma_{23}/\bar{\mu}_{11}, \end{gathered} \tag{5}$$

where $\nu$ is the dimensionless frequency. Here the displacement, $u_3^p$, and the nonzero (shear) stresses, $\sigma_{13} = \sigma_{31}$ and $\sigma_{23} = \sigma_{32}$, are rendered nondimensional and denoted by $w$ and $\tau_j$, $j = 1, 2$, respectively. In what follows, the corresponding (engineering) strains, $2\epsilon_{13} = 2\epsilon_{31}$ and $2\epsilon_{23} = 2\epsilon_{32}$, will be denoted by $\gamma_1$ and $\gamma_2$, respectively. The (normalized) field equations then become,

$$\tau_{1,1} + \tau_{2,2} + \nu^2\rho w = 0; \quad \tau_j = \mu_{jk}\gamma_k \quad (k \ summed), \tag{6}$$

$$\gamma_1 = w_{,1} \quad \gamma_2 = iQ_2 w, \quad w = w^p e^{iQ_1\xi_1}. \tag{7}$$

In view of equations (6, 7) and (2), the shear stress $\tau_2$ can be expressed in terms of $\tau_1$ and $w$, as follows:

$$\tau_2 = \frac{\mu_{12}}{\mu_{11}}\tau_1 + \frac{iQ_2}{D_{22}}w, \tag{8}$$

where $D_{22}$ is the corresponding component of the normalized elastic compliance matrix defined by,

$$\begin{pmatrix} D_{11} & D_{12} \\ D_{21} & D_{22} \end{pmatrix} = \frac{1}{\Delta}\begin{pmatrix} \mu_{22} & -\mu_{12} \\ -\mu_{21} & \mu_{11} \end{pmatrix}, \quad \Delta = \mu_{11}\mu_{22} - \mu_{12}^2.$$

Hence,

$$\tau_{2,2} = iQ_2\tau_2 = iQ_2\frac{\mu_{12}}{\mu_{11}}\tau_1 - \frac{{Q_2}^2}{D_{22}}w. \tag{9}$$

## 3. Variational Formulation: Layered Composites

Consider now the following functional:

$$I =< \tau_j, w_{,j} > + < w_{,j}, \tau_j > - < D_{jk}\tau_k, \tau_j > -\nu^2 < \rho w, w >, \qquad (10)$$

where $< gu, v >= \int_{-1/2}^{1/2} guv^* d\xi$ for a real-valued function $g(\xi)$ and complex-valued functions $u(\xi)$ and $v(\xi)$, with star denoting complex conjugate. In (10) $w$ and $\tau_j$ are viewed as independent fields subject to arbitrary variations. It is easy to show [29] that equations (6) are the Euler equations that render the functional $I$ stationary. For layered composites however, it is expedient to use (8) in (10) and consider $\tau_1$ and $w$ as the only independent fields subject to variations, especially since the periodicity in layered composites is only in one direction. Hence consider the functional,

$$\begin{aligned} I_1 =< \tau_1, w_{,1} > + < w_{,1}, \tau_1 > -iQ_2 < \frac{\mu_{12}}{\mu_{11}}\tau_1, w > +iQ_2 < \frac{\mu_{12}}{\mu_{11}}w, \tau_1 > \\ +Q_2^2 < \frac{1}{D_{22}}w, w > - < \frac{1}{\mu_{11}}\tau_1, \tau_1 > -\nu^2 < \rho w, w > . \end{aligned} \qquad (11)$$

The first variation of $I_1$ with respect to $w^*$ and $\tau_1^*$ yields, respectively,

$$\tau_{1,1} + [iQ_2\frac{\mu_{12}}{\mu_{11}}\tau_1 - \frac{Q_2^2}{D_{22}}w] + \nu^2\rho w = 0 \qquad \tau_1 = \mu_{11}w_{,1} + iQ_2\mu_{12}w, \qquad (12)$$

which also follow from (6, 7) and (8).

To find an approximate solution of the field equations (12) subject to the Bloch periodicity condition (2), consider the following estimates:

$$w = \sum_{\alpha=-N}^{+N} W^{(\alpha)} e^{i(Q_1+2\pi\alpha)\xi_1}, \quad \tau_1 = \sum_{\alpha=-N}^{+N} T^{(\alpha)} e^{i(Q_1+2\pi\alpha)\xi_1}, \qquad (13)$$

which automatically ensure the Bloch and continuity conditions.

Substitution into (11) now yields,

$$I_1 = \sum_{\alpha,\beta=-N}^{+N} \{T^{(\alpha)}[-i(Q_1+2\pi\alpha)]\delta_{\alpha\beta}W^{(\beta)*} + W^{(\alpha)}[+i(Q_1+2\pi\alpha)]\delta_{\alpha\beta}T^{(\beta)*}$$
$$-iQ_2T^{(\alpha)}\Lambda^{(\alpha\beta)}[\mu_{12}/\mu_{11}]W^{(\beta)*} + iQ_2W^{(\alpha)}\Lambda^{(\alpha\beta)}[\mu_{12}/\mu_{11}]T^{(\beta)*}$$
$$-T^{(\alpha)}\Lambda^{(\alpha\beta)}[1/\mu_{11}]T^{(\beta)*} + W^{(\alpha)}\Lambda^{(\alpha\beta)}[Q_2^2/D_{22} - \nu^2\rho]W^{(\beta)*}\}, \tag{14}$$

where $\Lambda^{(\alpha\beta)}$ is a linear integral operator, defined by

$$\Lambda^{(\alpha\beta)}[f(\xi)] = \int_{-1/2}^{1/2} f(\xi)e^{i2\pi(\alpha-\beta)\xi}d\xi = \int_{-1/2}^{1/2} f(\xi)e^{-i2\pi(\beta-\alpha)\xi}d\xi = \Lambda^{(\beta\alpha)^*}[f(\xi)], \tag{15}$$

with $f(\xi)$ being a real-valued integrable function.

For an even function, $f(\xi) = f(-\xi)$ (symmetric unit cells),

$$\Lambda^{(\alpha\beta)}[f(\xi)] = 2\int_0^{1/2} f(\xi)cos(2\pi(\alpha-\beta)\xi)d\xi = \Lambda^{(\beta\alpha)}[f(\xi)]. \tag{16}$$

Furthermore, for a piecewise constant $f(\xi)$, e.g.,

$$f(\xi) = \begin{cases} f_1 & 0 < \xi < l_1/2 \\ f_2 & l_1/2 < \xi < l_2/2 \\ ... & \\ ... & \\ f_n & l_{n-1}/2 < \xi < 1/2 \end{cases} \tag{17}$$

with $l_n = 1$, one obtains,

$$\Lambda^{(\alpha\beta)}[f(\xi)] = \begin{cases} \sum_{a=1}^{n} \frac{f_a - f_{a+1}}{\pi(\alpha-\beta)} sin(\pi(\alpha-\beta)l_a) & \alpha \neq \beta \\ \sum_{a=1}^{n}(f_a - f_{a+1})l_a = \bar{f} & \alpha = \beta, \quad f_{n+1} = 0. \end{cases}$$

(18)

Define an $M \times M$ matrix $\Lambda[f(\xi)] = [\Lambda^{(\alpha\beta)}][f(\xi)]$, $\alpha, \beta = 0, \pm 1, ..., \pm N$, and $M = 2N + 1$, and note that, in view of linearity, for any two constants $a_1$ and $a_2$,

$$a_1\Lambda[f_1(\xi)] + a_2\Lambda[f_2(\xi)] = \Lambda[a_1 f_1(\xi) + a_2 f_2(\xi)].$$

Also, let $H$ be an $M \times M$ diagonal matrix with components $(Q_1 + 2\pi\alpha)\delta_{\alpha\beta}$. Then, (14) can be rewritten as,

$$I_1 = \begin{bmatrix} W \\ T \end{bmatrix}^T \begin{bmatrix} Q_2^2\Lambda[1/D_{22}] - \nu^2\Lambda[\rho] & iH + Q_2\Lambda[\mu_{12}/\mu_{11}]\} \\ -iH + Q_2\Lambda[\mu_{12}/\mu_{11}]\} & -\Lambda[1/\mu_{11}] \end{bmatrix} \begin{bmatrix} W^* \\ T^* \end{bmatrix}. \quad (19)$$

For symmetric unit cells, $I_1$ may be written as,

$$I_{1s} = \begin{bmatrix} W^* \\ T^* \end{bmatrix}^T \begin{bmatrix} Q_2^2\Lambda[1/D_{22}] - \nu^2\Lambda[\rho] & -iH + Q_2\Lambda[\mu_{12}/\mu_{11}]\} \\ iH + Q_2\Lambda[\mu_{12}/\mu_{11}]\} & -\Lambda[1/\mu_{11}] \end{bmatrix} \begin{bmatrix} W \\ T \end{bmatrix}. \quad (20)$$

Furthermore, when $\mu_{12} = 0$, we obtain,

$$I_2 = \begin{bmatrix} W^* \\ T^* \end{bmatrix}^T \begin{bmatrix} Q_2^2\Lambda[\mu_{22}] - \nu^2\Lambda[\rho] & -iH \\ iH & -\Lambda[1/\mu_{11}] \end{bmatrix} \begin{bmatrix} W \\ T \end{bmatrix}. \quad (21)$$

Note that, in view of equation (16), $\Lambda[f(\xi)]$ in (19) and (21) is real-valued for symmetric unit cells. Furthermore, when a symmetric unit cell consists of layers of uniform elasticities and densities, equation (18) gives $\Lambda^{(\alpha\beta)}[f(\xi)]$ explicitly.

Now, minimization of $I_2$ (or $I_1$ for $\mu_{12} \neq 0$) with respect to the unknown coefficients $W^{(\alpha)}$ and $T^{(\alpha)}$, results in an eigenvalue problem which yields the band structure of the composite for anti-plane Bloch-form shear waves,

$$\left[(I + Q_2^2 A\Lambda[\mu_{22}]) - \nu^2 A\Lambda[\rho]\right] W = 0, \qquad A = H^{-1}\Lambda[1/\mu_{11}]H^{-1}, \quad (22)$$

where $\mathbf{I}$ is the identity matrix. For given values of $Q_1$ and $Q_2$, the eigenvalues, $\nu$, of equation$(22)_1$ are obtained from

$$det\left|(I + Q_2^2 A\Lambda[\mu_{22}]) - \nu^2 A\Lambda[\rho]\right| = 0, \tag{23}$$

and for each eigenvalue, the corresponding displacement field, $W$, is given by $(22)_1$, and the stress field by

$$T = i\{\Lambda[1/\mu_{11}]\}^{-1} HW. \tag{24}$$

Note that $H$ is a diagonal matrix whose components are linear in $Q_1$.

From (6, 7)), the $x_2$-component of the shear stress, $\tau_2$, and the $x_1$-component of the shear strain, $\gamma_1$, are given by,

$$\tau_2 = iQ_2\mu_{22}(\xi_1)\sum_{\alpha=-N}^{+N} W^{(\alpha)} e^{i(Q_1+2\pi\alpha)\xi_1}, \quad \gamma_1 = D_{11}(\xi_1)\sum_{\alpha=-N}^{+N} T^{(\alpha)} e^{i(Q_1+2\pi\alpha)\xi_1}. \tag{25}$$

As can be seen, $W$ is real-valued and $T$ is purely imaginary. Both are implicit functions of $Q_1$ and $Q_2$.

The periodic parts of the displacement, velocity, and stress-components are summarized here for subsequent application,

$$w^p(\xi_1) = \sum_{\alpha=-N}^{+N} W^{(\alpha)} e^{i2\pi\alpha\xi_1}, \quad \dot{w}^p(\xi_1) = -i\nu\sum_{\alpha=-N}^{+N} W^{(\alpha)} e^{i2\pi\alpha\xi_1}, \tag{26}$$

$$\tau_1^p(\xi_1) = \sum_{\alpha=-N}^{+N} T^{(\alpha)} e^{i2\pi\alpha\xi_1}, \quad \tau_2^p(\xi_1) = iQ_2\sum_{\alpha=-N}^{+N} W^{(\alpha)}\mu_{22}(\xi_1) e^{i2\pi\alpha\xi_1}, \tag{27}$$

where for each frequency band $J$, associated with an eigenvalue $\nu_J$, equations (22, 24) yield the corresponding coefficients, $W_J^{(\alpha)}$ and $T_J^{(\alpha)}$; the subscript $J$ has been omitted in the above expressions. Once $W^{(\alpha)}$ and $T^{(\alpha)}$ are calculated for a desired eigenvalue, $\nu$, the above expressions give the periodic part of the field variables.

## 4. Phase and Group Velocities, and Energy Flux

For a given (symmetric) unit cell that consists of a given number of layers of prescribed mass densities and stiffnesses, matrices $A$ and $\Lambda[f(\xi)]$ in (22) can be computed explicitly using (16). The expression in the left-hand side of (23) will then depend parametrically on the wave-vector components, $Q_1$ and $Q_2$. The resulting eigenfrequencies, $\nu$, can thus be expressed as functions of $Q_1$ and $Q_2$. These eigenfrequencies form surfaces in the ($Q_1$, $Q_2$, $\nu$)-space, referred to as phase constant surfaces (or dispersion surfaces). The first zone corresponds to $-\pi \leq Q_1, Q_2 \leq \pi$. We focus on this zone and examine the dynamic properties of layered elastic composites on the first and second frequency bands.

On each frequency band, the phase and group velocities are given by,

$$v^p_{Jk} = \frac{\nu_J Q_k}{Q_1^2 + Q_2^2} \quad v^g_{Jk} = \frac{\partial \nu_J}{\partial Q_k}, \quad k = 1, 2; \tag{28}$$

here and below, $J = 1, 2, ...$ denotes the frequency band and $k = 1, 2$, the $x_1$- and the $x_2$-directions, respectively. The group velocity defines the direction of the energy flux; it is given by

$$\alpha_J = atan(\frac{v^g_{J2}}{v^g_{J1}}). \tag{29}$$

The $x_1$- and $x_2$-components of the energy-flux vector are given by

$$E_{Jk} = \frac{\nu_J}{2\pi} \int_0^{\frac{2\pi}{\nu_J}} < Re(\tau_{Jk}(\xi_1, \xi_2, t)) Re(\dot{w}^*_J(\xi_1, \xi_2, t)) > dt = -\frac{1}{2} < \tau^p_{Jk} \dot{w}^{p*}_J >, \tag{30}$$

which is real-valued, where $k = 1, 2$. Substitution from (26, 27) results in,

$$E_{J1} = -\frac{1}{2} i \nu_J \sum_{\alpha=-M}^{+M} T^{(\alpha)}_J W^\alpha_J, \quad E_{J2} = \frac{1}{2} \nu_J Q_2 \sum_{\alpha,\beta=-M}^{+M} W^{(\alpha)}_J W^{(\beta)}_J \Lambda^{(\alpha\beta)}[\mu_{22}]. \tag{31}$$

The direction, $\beta_J$, of the energy-flux vector is hence given by,

$$\beta_J = atan(\frac{E_{J2}}{E_{J1}}). \tag{32}$$

It is known [7] that the direction, $\alpha_J$, is essentially the same as the direction $\beta_J$ of the energy flux for nondissipative media. We shall illustrate this in what follows.

**An Important Cautionary Note:** For an oblique anti-plane shear wave in a periodic layered elastic composite, the angle of incidence $\theta = atan(\frac{Q_2}{Q_1})$ cannot be arbitrary, limiting the admissible values of $Q_2$ depending on the structure and composition of the corresponding unit cell, as well as on values of $Q_1$.

## 5. Illustrative Examples

### *5.1. Example 1: A Two-Phase Composite*

We now examine the dynamic response of a *two-phase* composite where the corresponding unit cell consists of a very stiff and a relatively soft layer; see Figure 1. We show that, on the second frequency pass-band of such composites, the group and phase velocities in the $x_1$-direction (normal to layers) are antiparallel (*backward wave*), whereas they are parallel in the $x_2$-direction (parallel to layers), signifying *the negative-energy refraction with positive phase refraction* characteristic of this class of elastic composites in anti-plane shearing. In contrast, on the first frequency pass-band of the composite, the group and phase velocities are parallel, both in the $x_1$- and $x_2$-directions.

While the formulation and calculations are in terms of dimensionless quantities, in what follows the results are presented in terms of dimensional

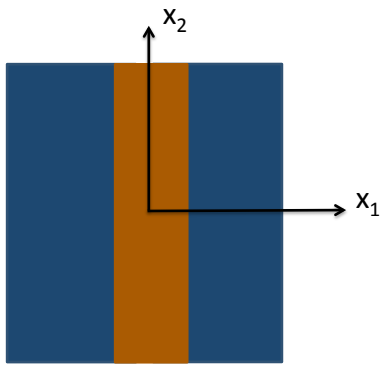


Figure 1: The unit cell of a two-phase composite.

values for the symmetric unit cell shown in Figure 1. The dimensionless parameters and the results are calculated using the following specific material properties (typical for PMMA and steel):

1. $\mu_1 = 80 \times 10^9$ Pa; $\rho_1 = 8000$ kg/m$^3$; total thickness = 1.3mm
2. $\mu_2 = 3 \times 10^9$ Pa; $\rho_2 = 1180$ kg/m$^3$; total thickness = 3mm.

The unit cell is 4.3 mm thick. The resulting dimensionless parameters used in the calculations have the following values:

1. $\bar{\mu}_1 = 3.0442$; $\bar{\rho}_1 = 2.4677$; $\bar{h}_2 = 0.3023$
2. $\bar{\mu}_2 = 0.1142$; $\bar{\rho}_2 = 0.3640$; $\bar{h}_1 = 0.6977$.

The layers are isotropic, and subscripts $1, 2$ identify the properties ($\mu$ for shear modulus and $\rho$ for density) of each layer within the unit cell. For example, $\mu_2$ stands for $\mu_{11} = \mu_{22}$ of layer 2. The superimposed bar denotes the corresponding normalized value; see equations (4, 5). To obtain the frequency in kHz, and the group velocity, $v^g_{Jk}$, in m/s, multiply $\nu$ by 105, and $v^g_{Jk}$ by 2847, respectively.

*5.1.1. Frequency Band Structure*

Now examine the variation of the frequency as a function of the wave-vector components, $Q_1$ and $Q_2$. For each pair of $Q_1$ and $Q_2$, the direction of the wave vector is obtained from $\theta = atan(Q_2/Q_1)$, the direction of the group-velocity vector from $\alpha_J = atan(v^g_{J2}/v^g_{J1})$ (which is shown below to be the same as that of the energy-flux vector, $\beta_J = atan(E_{J2}/E_{J1})$), and the direction of the phase-velocity from $\phi_J = atan(v^p_{J2}/v^p_{J1}) = \theta$, respectively.

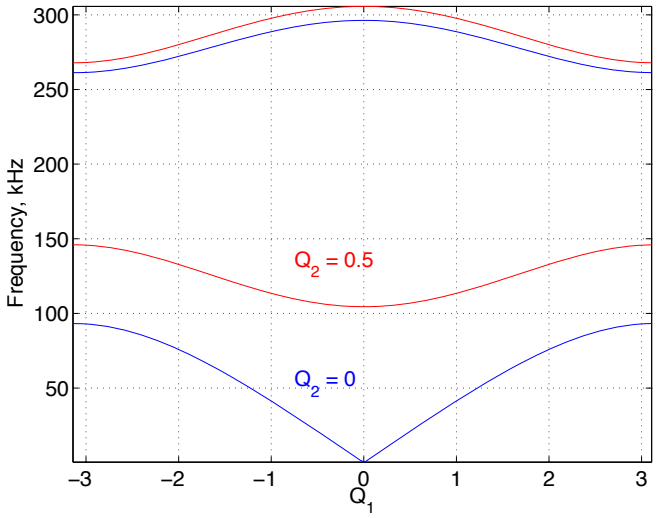


Figure 2: Frequency (in kHz) as function of $Q_1$ for indicated values of $Q_2$; two-phase composite.

Figure 2 shows the frequency (in kHz) as a function of $Q_1$ for indicated values of $Q_2$, and Figures 3(a, b) show the constant-frequency contours together with the direction of energy flow (superimposed arrows) as functions of $Q_1$ and $Q_2$, for the first two frequency pass-bands . As is seen, for suitably small values of $Q_2$ these contours are ellipses on the first pass-band whereas they

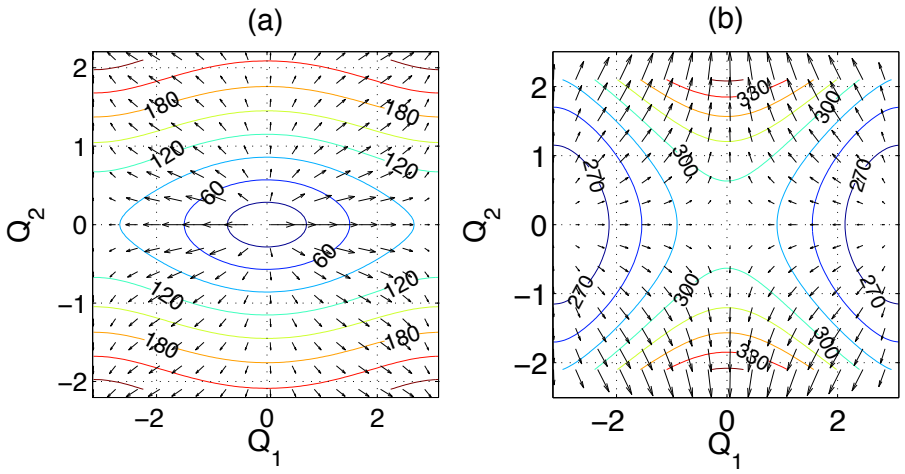


Figure 3: Contours of constant frequency (in kHz) and group-velocity vectors for: (a) first pass band, and (b) second pass band; two-phase composite; (for clarity, in graph (a) the $x_2$-component of the group velocity is reduced by a factor of 5).

are hyperbolae on the second pass-band. On the first frequency pass-band, the corresponding components of the energy-flux and the phase-velocity vectors are parallel, but not on the second frequency pass-band. In this latter case, the energy flux in the $x_1$-direction is antiparallel with the corresponding component of the phase-velocity, while in the $x_2$-direction these components are parallel. Hence the composite may or may not display *negative refraction*, depending on the direction of the incident wave, as shown in Figures 3($b$). Here in addition, *negative energy refraction is accompanied by positive phase refraction* and *positive energy refraction is accompanied by negative phase refraction*; see subsection 5.2 for illustration. In terms of the group and phase velocities, in Figure 3(a), $v_1^g v_1^p > 0$ and $v_2^g v_2^p > 0$, whereas in Figure 3(b), $v_1^g v_1^p < 0$ but $v_2^g v_2^p > 0$.

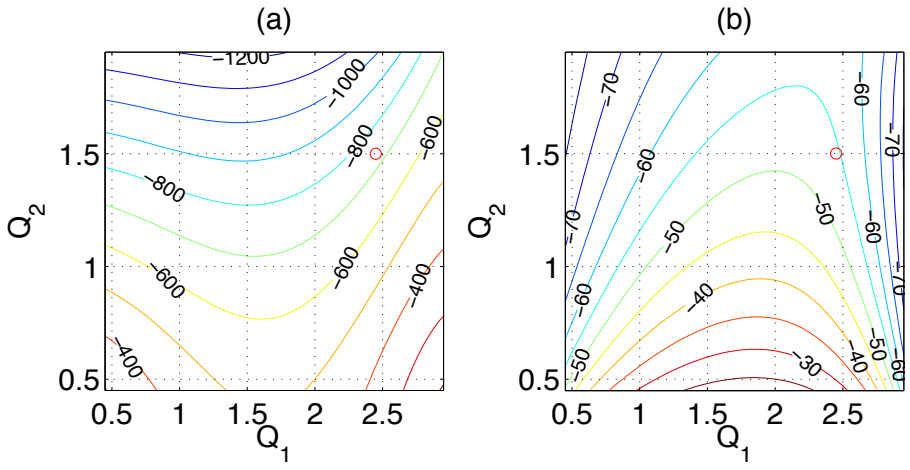


Figure 4: (a) Contours of constant group velocity (in m/s), and (b) contours of constant (energy) refraction angle; for second pass-band of a two-phase composite (negative sign signifies a negative angle with the $x_1$-axis). The red circles correspond to values for Example 2 discussed in subsection 5.2.

Focusing on the second frequency pass-band, we have presented in Figure 4(a) contours of constant group velocity (in m/s) and in Figure (4b) those of constant (energy-flux) refraction angle. As pointed out above, the group-velocity vectors are oriented in the direction of the energy flow. For positive wave-vector components, they have negative components in the $x_1$-direction but positive components in the $x_2$-direction; this is signified by negative signs in Figures 4(a, b).

As is mentioned before, the group velocity-vector defines the direction of energy flux. Figures (5a, b) show the refraction angles, ( $\alpha_1$ and $\beta_1$) and ($\alpha_2$ and $\beta_2$), as functions of the frequency for $\theta = atan(\frac{Q_2}{Q_1}) = 10, 30^o$. The solid curves correspond to the energy-flux and the open circles to the group-velocity directions. The figures show that the orientations of the group-

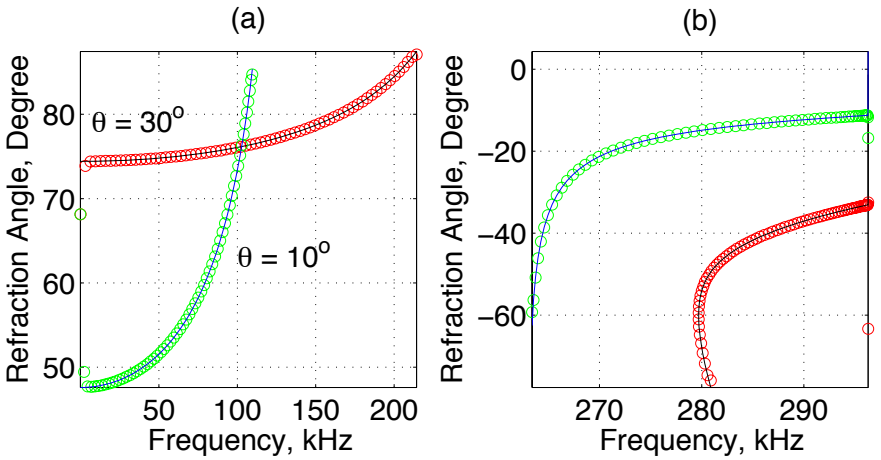


Figure 5: Refraction angle for indicated incident angles as functions of frequency; solid (black: $30^o$; blue: $10^o$) curves are energy-flux and open (red: $30^o$; green: $10^o$) circles are for group-velocity direction; (a) first frequency pass-band, and (b) second frequency pass-band.

velocity and energy-flux vectors are essentially indistinguishable.

### *5.2. Example 2: Negative Refraction with Positive Phase Velocity and Positive Refraction with Negative Phase Velocity*

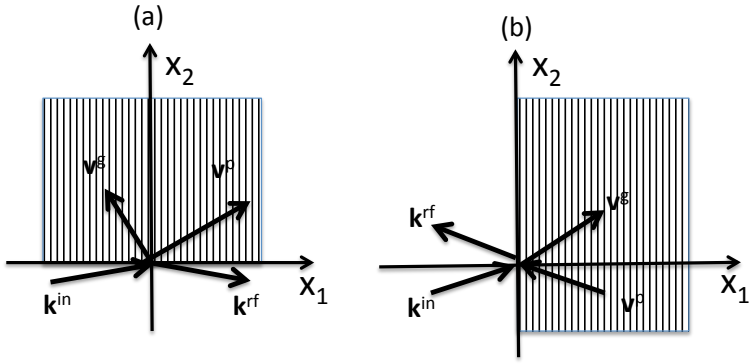


Figure 6: Plane harmonic wave of wave vector $\mathbf{k}^{in}$ is incident from (a) the $x_2 < 0$ and (b) the $x_1 < 0$ homogeneous half-space toward a periodic half-space; $\mathbf{k}^{rf}$ and $\mathbf{k}^{tr}$ are the reflected and transmitted wave vectors; $\mathbf{v}^g$ and $\mathbf{v}^p$ are the corresponding group and phase velocities.

Examination of Figure 3 readily reveals that the layered composite can display negative refraction or negative phase-velocity refraction depending on how it is interfaced with a homogeneous solid. Figures 6(a,b) suggest two possible ways. In Figure 6(a), the layered composite occupies the half-space $x_2 > 0$ while a homogeneous solid (say, aluminum) is occupying the half-space $x_2 < 0$, whereas in Figure 6(b) the interface of the layered medium and aluminum is along the $x_2$-axis on the $x_1 = 0$-axis. In each case, a plane harmonic anti-plane shear wave of wave-vector $\mathbf{k}^{in}$ is incident from the homogeneous solid toward the interface at an incident angle $\theta_0$, where

$\theta = 10^o$ in Figure 3(a) and $\theta = 20^o$ in Figure 6(b). In the first case, negative refraction is accompanied by positive phase refraction, and in the second case this is reversed, namely positive refraction is accompanied by negative phase refraction.

Let $C_0$ be the shear-wave velocity in the homogeneous solid. Consider Figure 6(a) and note that,

$$Q_1 = Q_1^{rf} = Q_1^{tr} = \frac{cos(\theta_0)}{\bar{C}_0}\nu, \quad Q_2 = -Q_2^{rf} = \frac{sin(\theta_0)}{\bar{C}_0}\nu, \quad \bar{C}_0 = C_0\sqrt{(}\bar{\rho}/\bar{\mu}_{11}), \tag{33}$$

where $\bar{C}_0$ is the dimensionless value of the shear-wave speed in the homogeneous $x_2 < 0$ half-space. For a given frequency, say $\nu_0$, $Q_1^{tr}$ is given by $(33)_1$ and $Q_2^{tr}$ is calculated such that $\nu(Q_1^{tr}, Q_2^{tr}) = \nu_0$. For aluminum with a shear-wave speed of $C_0 = 3{,}040$ m/s and $\theta_0 = 10^o$, Figure (7) shows the variation of the frequency in kHz for $2.2 < Q_1 < 2.7$ and $1.2 < Q_2 < 1.8$. For a frequency $\cong$ 281.9 kHz ($\nu \cong 2.67$), we have $Q_1^{tr} = Q_1 \cong 2.47$, and $Q_2^{tr} = 1.50$. This gives a refraction angle of about -54.4$^o$ and a group velocity of $\cong$ 733.5 m/s. These values are identified in Figures 4 and 7 by red circles.

Now consider Figure 6(b) and note that the phase angle $Q_2\xi_2 - \nu t$ on the $x_1 = 0$-axis must be continuous. Hence,

$$Q_2 = Q_2^{rf} = Q_2^{tr} = \frac{sin(\theta_0)}{\bar{C}_0}\nu, \quad Q_1 = -Q_1^{rf} = \frac{cos(\theta_0)}{\bar{C}_0}\nu. \tag{34}$$

For $\theta = 20^o$ and a frequency $\cong$ 280 kHz ($\nu \cong 2.65$), we have $Q_2^{tr} = Q_2 \cong 0.85$, and $Q_1^{tr}$ = -1.50. This gives a refraction angle of about 37.3$^o$ and a group velocity of $\cong$ 608.9 m/s.

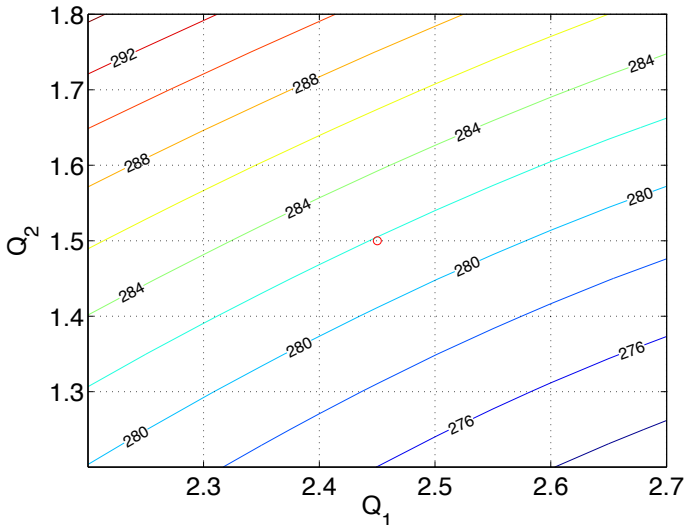


Figure 7: Contours of constant frequency (in kHz) for $2.4 < Q_1 < 2.6$ and $1.2 < Q_2 < 1.8$; second frequency pass-band.

### *5.3. Example 4: A Three-Phase Composite*

Qualitatively, the three-phase layered composite has the same dynamic response as the two-phase composite considered above. As an illustration, consider a unit cell consisting of a central 1 mm thick layer of steel that is sandwiched by two layers of a polyurea/phenolic-microballoon composite of 0.4 mm thickness each, and then by two layers of PMMA of 1.25 mm each, the total thickness of the unit cell being 4.3 mm, the same as the two-phase composite.

Figures (8a, b) display contours of constant frequency (in kHz) for the first (a) and the second (b) frequency pass-bands together with a representative number of group-velocity vectors; for clarity, the $x_2$-components of these vectors are reduced by a factor of 10. For suitably small values of $Q_2$, these

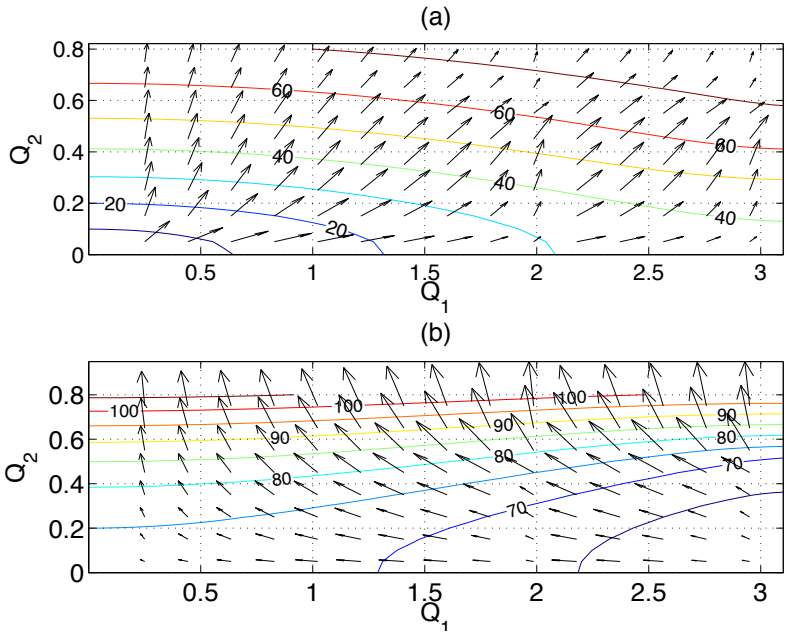


Figure 8: Contours of constant frequency (kHz): (a) first pass band, (b) second pass band, together with typical group-velocity vectors; the $x_2$-components of the group-velocity vectors are reduced by a factor of 10, and arrows are scaled for clarity; (three-phase unit cell).

contours are ellipses for the first pass-band, but they are hyperbolae for the second pass-band. Moreover, both of the components of the group-velocity vectors are parallel with the corresponding phase-velocity components on the first pass-band, but on the second frequency pass-band, only their $x_2$-components are parallel while their $x_1$-components are antiparallel with the corresponding components of the phase-velocity vectors. Hence, the refraction properties here are the same as those of the two-phase composites; see Figures (6). Also, the direction of the group-velocity and and energy-flux vectors are the same.

Hence, in general for anti-plane shear waves, layered periodic composites display *negative refraction accompanied by positive phase-velocity refraction and positive refraction accompanied by negative phase-velocity refraction* depending how they are interfaced with a homogeneous material.

### *5.4. Extension to Two-dimensional Unit Cells*

Here we briefly outline how the results can easily be extended to two-dimensional periodic composites, assuming for simplicity square unit cells of dimensions $a_1 = a_2 = a$.

The displacement $w$ and the stresses $\tau_j$ are now expressed as

$$\begin{bmatrix} w \\ \tau_j \end{bmatrix} = \sum_{n_1,n_2=-N}^{+N} \begin{bmatrix} W^{(n_1,n_2)} \\ T_j^{(n_1,n_2)} \end{bmatrix} e^{i[(Q_1+2\pi n_1)\xi_1+(Q_2+2\pi n_2)\xi_2]-\nu t)}, \tag{35}$$

where $\xi_j = x_j/a$, $Q_j = k_j/a$ (no sum on $j$, $j = 1, 2$), and $\nu$ is the dimensionless frequency. Substitution into (10) and minimization with respect to the

unknown coefficients $W$ and $T_j$ results in

$$\begin{bmatrix} iH_1 & iH_2 & \nu^2\Lambda_\rho \\ \Lambda_{D_{11}} & 0 & -iH_1 \\ 0 & \Lambda_{D_{22}} & -iH_2 \end{bmatrix} \begin{bmatrix} T_1 \\ T_2 \\ W \end{bmatrix} = 0, \tag{36}$$

where $\Lambda_f = [\Lambda_f^{(n_1 n_2, m_1 m_2)}]$ is an $M^2 \times M^2$ matrix, and $H_1$ and $H_2$ are two $M^2 \times M^2$ diagonal matrices with the respective components $(Q_1 + 2\pi n_1)\delta_{n_1 m_1}$ and $(Q_2 + 2\pi n_2)\delta_{n_2 m_2}$. The components of $\Lambda_f$ are defined by

$$[\Lambda_f] = \int_{-1/2}^{1/2} \int_{-1/2}^{1/2} f(\xi_1, \xi_2) e^{i2\pi[(n_1 - m_1)\xi_1 + (n_2 - m_2)\xi_2]} d\xi_1 d\xi_2, \tag{37}$$

with $f(\xi_1, \xi_2)$ being a real-valued integrable function.

From the system of linear and homogeneous equations (36),we obtain,

$$\left[\Phi - \nu^2\Lambda_\rho\right] W = 0, \quad \Phi = (H_1 \Lambda_{D_{11}}^{-1} H_1 + H_2 \Lambda_{D_{22}}^{-1} H_2). \tag{38}$$

For given values of $Q_1$ and $Q_2$, the eigenvalues, $\nu$, of equation$(38)_1$ are obtained from

$$det\left|\Phi - \nu^2\Lambda_\rho\right| = 0, \tag{39}$$

and for each eigenvalue, the corresponding displacement vector $W$, is given by $(38)_1$, and the stress components by

$$T_1 = i\Lambda_{D_{11}}^{-1} H_1 W, \qquad T_2 = i\Lambda_{D_{22}}^{-1} H_2 W. \tag{40}$$

The results outlined above can be modified to obtain the necessary equations when theplane-wave expansion method is used. For this, equation $(38)_2$ needs to be changed to $\Phi = (H_1 \Lambda_{\mu_{11}} H_1 + H_2 \Lambda_{\mu_{22}} H_2)$. This means that $f(\xi_1, \xi_2)$ now stands for the (spatially variable) shear modulus of the unit cell.

The calculation of the group-velocity and energy-flux vectors follows the same procedure as outlined in section (4), with the energy-flux being given by equation (30). In what follows, a two-dimensional illustrative example is briefly discussed.

### *5.5. A Two-dimensional Illustration*

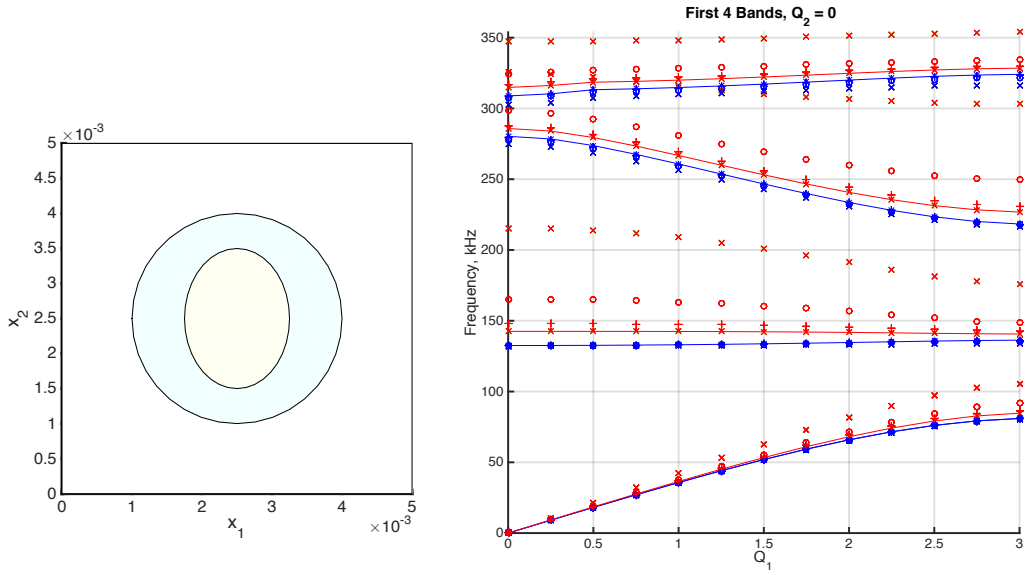


Figure 9: A 3-phase doubly periodic composite: (Left) cross-section of unit cell with polymer coated elliptical central steel rods embedded in PMMA matrix; (Right) first 4 frequency pass-bands (in kHz), comparing the results of the present method (in blue) with those of the plane-wave expansion method (in red) for 49- (crosses, x), 169- (open circles, o), 441- (pluses, +), 729- (dots, .), and 961- (solid lines, -) term series solutions.

Consider a periodic composite consisting of a two-dimensional square arrangement of steel rods of a common elliptical cross-section (1.5 by 2.0 mm),

coated by an elastomeric polymer (0.7 GPa shear modulus, 1000 kg/m$^3$ mass-density) of outer 3.0 mm diameter, and embedded within a PMMA matrix, as shown in Figure (9, Left); the properties of steel and PMMA are given in subsection (5.1). In Figure (9, Right), we have compared our results with those obtained using the plane-wave expansion method for $N = 6, 10, 13, 15$, corresponding to 49,169, 441, 729 and 961 terms, where the plane-wave expansion results are in red and those for the present variational method are in blue. As can be seen, our method converges very rapidly, yielding essentially the final results for $N = 3$ (49 terms), whereas the plane-wave expansion has not yet converged even for several hundred terms.

As our final illustration, Figures (10) show the equifrequency contours of the first two bands together with the superimposed energy-flux vectors, which reveal a wealth of physics for this two-dimensional phononic crystal; for thorough exposition, discussions, and several examples, see [30].

*5.6. Discussion and Conclusions*

Periodic elastic composites can be designed to have static and dynamic characteristics that are not shared by their constituent materials. Some of the dynamic characteristics and responses of layered periodic composites are explored in this work, using harmonic anti-plane shear waves. The considered layered composites lack periodicity in the direction parallel to the layers. This profoundly affects their dynamic response, leading to anomalous wave-refraction, namely, for this class of composites, negative refraction is accompanied by positive phase-velocity refraction. This phenomenon was first recognized by [11] for TM and TE electromagnetic waves in photonic crystals. Here, we have shown this in phononic crystals and, in addition,

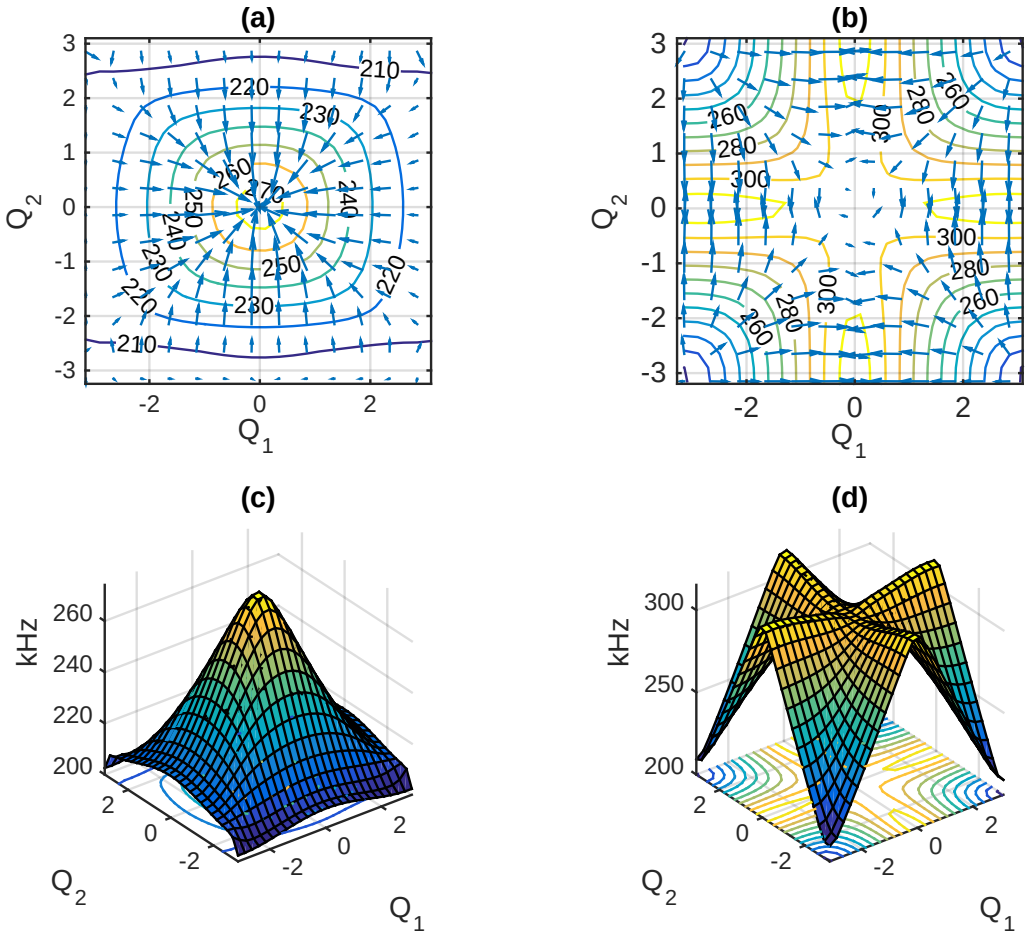


Figure 10: The third and fourth pass bands: (a and b) equifrequency contours, and (c and d) the corresponding energy-flux vectors; 3-phase doubly periodic composite

we have shown that the composite can also display negative phase-velocity refraction accompanied by positive energy refraction, a phenomenon which does not seem to have been recognized before.

In the present work, a general variational approach is developed that produces the entire band structure of the composite for unit cells of any number of layers with any arbitrary properties. Explicit expressions are developed for the band structure, group-velocity and energy-flux vectors. The general results are illustrated using a two-phase and a three-phase unit cell with piecewise constant properties. The presented method is applicable and effective also when some or all of the layers in a unit cell have spatially varying properties. We have also shown that the method can easily be extended to two-dimensional unit cells, and have illustrated this using a three-phase doubly periodic example. By comparing results of our method with those obtained using the plane-wave expansion approach, we have demonstrated the remarkable effectiveness of our general variational formulation.

## 6. Data Accessibility

This paper is theoretical and includes in the text all necessary equations to support the accompanying calculations. There are no data set.

## 7. Competing Interests

I have no competing interests.

## 8. Authors Contributions

This is a single-author-paper. All work that is presented in this paper is carried out by its indicated author.

## 9. Acknowledgments

This research has been conducted at the Center of Excellence for Advanced Materials (CEAM) at the University of California, San Diego.

## 10. Funding Source

From DOD, DARPA RDECOM W91CRB-10-1-0006 to the University of California, San Diego.

## 11. References

[1] Mats Åberg and Peter Gudmundson. The usage of standard finite element codes for computation of dispersion relations in materials with periodic microstructure. *The Journal of the Acoustical Society of America*, 102:2007, 1997.

[2] Jacob Aboudi. Harmonic waves in composite materials. *Wave motion*, 8(4):289–303, 1986.

[3] Ivo Babuška and JE Osborn. Numerical treatment of eigenvalue problems for differential equations with discontinuous coefficients. *Mathematics of Computation*, 32(144):991–1023, 1978.

[4] Leon Y Bahar. Transfer matrix approach to layered systems. *Journal of the Engineering Mechanics Division*, 98(5):1159–1172, 1972.

[5] Biswajit Banerjee. *An Introduction to Metamaterials and Waves in Composites*. CRC Press, 2011.

[6] Arthur MB Braga and George Herrmann. Floquet waves in anisotropic periodically layered composites. *The Journal of the Acoustical Society of America*, 91:1211, 1992.

[7] L Brillouin. Wave guides for slow waves. *Journal of Applied Physics*, 19(11):1023–1041, 1948.

[8] Richard M Christensen. *Mechanics of composite materials*. DoverPublications. com, 2012.

[9] B Djafari-Rouhani and Léonard Dobrzynski. Simple excitations in n-layered superlattices. *Solid state communications*, 62(9):609–615, 1987.

[10] SI Fomenko, MV Golub, Ch Zhang, TQ Bui, and Y-S Wang. In-plane elastic wave propagation and band-gaps in layered functionally graded phononic crystals. *International Journal of Solids and Structures*, 51(13):2491–2503, 2014.

[11] R Gajic, R Meisels, F Kuchar, and K Hingerl. Refraction and rightness in photonic crystals. *Optics express*, 13(21):8596–8605, 2005.

[12] Freeman Gilbert and George E Backus. Propagator matrices in elastic wave and vibration problems. *Geophysics*, 31(2):326–332, 1966.

[13] Cécile Goffaux and José Sánchez-Dehesa. Two-dimensional phononic crystals studied using a variational method: Application to lattices of locally resonant materials. *Physical Review B*, 67(14):144301, 2003.

[14] Cécile Goffaux, José Sánchez-Dehesa, and Philippe Lambin. Comparison of the sound attenuation efficiency of locally resonant materials and elastic band-gap structures. *Physical Review B*, 70(18):184302, 2004.

[15] W Anthony Green. Reflection and transmission phenomena for transient stress waves in fiber composite laminates. In *Review of Progress in Quantitative Nondestructive Evaluation*, pages 1407–1414. Springer, 1991.

[16] Bernard Hosten and Michel Castaings. Transfer matrix of multilayered absorbing and anisotropic media. measurements and simulations of ultrasonic wave propagation through composite materials. *The Journal of the Acoustical Society of America*, 94:1488, 1993.

[17] J A Kohn, W Krumhansl and E H Lee. Variational methods for dispersion relations and elastic properties of composite materials. *Journal of Applied Mechanics*, 39(2):327–336, 1972.

[18] Philippe Langlet, Anne-Christine Hladky-Hennion, and Jean-Noël Decarpigny. Analysis of the propagation of plane acoustic waves in passive periodic materials using the finite element method. *The Journal of the Acoustical Society of America*, 98:2792, 1995.

[19] Ismo V Lindell, SA Tretyakov, KI Nikoskinen, and S Ilvonen. Bw me-

dia with negative parameters, capable of supporting backward waves. *Microwave and Optical Technology Letters*, 31(2):129–133, 2001.

[20] AK Mal. Wave propagation in layered composite laminates under periodic surface loads. *Wave Motion*, 10(3):257–266, 1988.

[21] Graeme W Milton and John R Willis. On modifications of newton's second law and linear continuum elastodynamics. *Proceedings of the Royal Society A: Mathematical, Physical and Engineering Science*, 463(2079):855–880, 2007.

[22] S Minagawa and S Nemat-Nasser. Harmonic waves in three-dimensional elastic composites. *International Journal of Solids and Structures*, 12(11):769–777, 1976.

[23] S Minagawa, S Nemat-Nasser, and M Yamada. Finite element analysis of harmonic waves in layered and fibre-reinforced composites. *International Journal for Numerical Methods in Engineering*, 17(9):1335–1353, 1981.

[24] Adnan H Nayfeh. The general problem of elastic wave propagation in multilayered anisotropic media. *The Journal of the Acoustical Society of America*, 89:1521, 1991.

[25] Adnan H Nayfeh. *Wave propagation in layered anisotropic media: With application to composites*. Access Online via Elsevier, 1995.

[26] S Nemat-Nasser. General variational methods for waves in elastic composites. *Journal of Elasticity*, 2(2):73–90, 1972.

[27] S Nemat-Nasser. Harmonic waves in layered composites. *Journal of Applied Mechanics*, 39:850, 1972.

[28] S Nemat-Nasser. Discussion: Variational methods for dispersion relations and elastic properties of composite materials. *Journal of Applied Mechanics*, 40(1):327–336, 1973.

[29] S Nemat-Nasser, FCL Fu, and S Minagawa. Harmonic waves in one-, two-and three-dimensional composites: bounds for eigenfrequencies. *International Journal of Solids and Structures*, 11(5):617–642, 1975.

[30] Sia Nemat-Nasser. Refraction characteristics of phononic crystals. *arXiv preprint arXiv:1412.4019*, 2014.

[31] Sia Nemat-Nasser and Muneo Hori. *Micromechanics: overall properties of heterogeneous materials*, volume 2. Elsevier Amsterdam, 1993, 1999.

[32] Sia Nemat-Nasser and Ankit Srivastava. Overall dynamic constitutive relations of layered elastic composites. *Journal of the Mechanics and Physics of Solids*, 59(10):1953–1965, 2011.

[33] Sia Nemat-Nasser, John R Willis, Ankit Srivastava, and Alireza V Amirkhizi. Homogenization of periodic elastic composites and locally resonant sonic materials. *Physical Review B*, 83(10):104103, 2011.

[34] AA Oliner and T Tamir. Backward waves on isotropic plasma slabs. *Journal of Applied Physics*, 33(1):231–233, 1962.

[35] SI Rokhlin and L Wang. Stable recursive algorithm for elastic wave

propagation in layered anisotropic media: Stiffness matrix method. *The Journal of the Acoustical Society of America*, 112:822, 2002.

[36] SaM Rytov. Acoustical properties of a thinly laminated medium. *Sov. Phys. Acoust*, 2:68–80, 1956.

[37] Mihail Sigalas, Manvir S Kushwaha, Eleftherios N Economou, Maria Kafesaki, Ioannis E Psarobas, and Walter Steurer. Classical vibrational modes in phononic lattices: theory and experiment. *Zeitschrift für Kristallographie*, 220(9-10):765–809, 2005.

[38] Ankit Srivastava and Sia Nemat-Nasser. On the limit and applicability of dynamic homogenization. *Wave Motion*, 2014.

[39] William T Thomson. Transmission of elastic waves through a stratified solid medium. *Journal of Applied Physics*, 21:89, 1950.

[40] John R Willis. Variational and related methods for the overall properties of composites. *Advances in applied mechanics*, 21:1–78, 1981.

[41] John R Willis. Variational principles for dynamic problems for inhomogeneous elastic media. *Wave Motion*, 3(1):1–11, 1981.

[42] John R Willis. Some thoughts on dynamic effective properties–a working document. *arXiv preprint arXiv:1311.3875*, 2013.

[43] John R Willis. A study of obliquely propagating longitudinal shear waves in a periodic laminate. *arXiv preprint arXiv:1310.6561*, 2013.